



Modeling the CH Stretch Vibrational Spectroscopy of $M^+[\text{Cyclohexane}]$ ($M = \text{Li}, \text{Na}, \text{and K}$) Ions

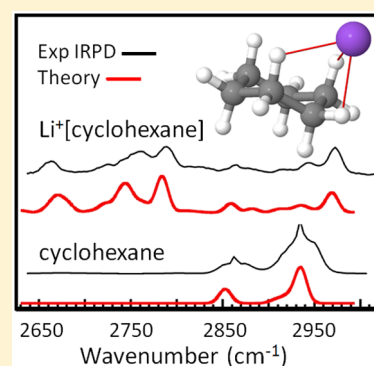
Published as part of *The Journal of Physical Chemistry A* virtual special issue "Spectroscopy and Dynamics of Medium-Sized Molecules and Clusters: Theory, Experiment, and Applications".

Edwin L. Sibert III,^{*,†} Daniel P. Tabor,[†] and James M. Lisy[‡]

[†]Department of Chemistry and Theoretical Chemistry Institute, University of Wisconsin—Madison, Madison, Wisconsin 53706, United States

[‡]Department of Chemistry, University of Illinois at Urbana—Champaign, Urbana, Illinois 61801, United States

ABSTRACT: The CH stretch vibrations of $M^+[\text{cyclohexane}][\text{Ar}]$ ($M = \text{Li}, \text{Na}, \text{and K}$) cluster ions were theoretically modeled. Results were compared to the corresponding infrared photodissociation spectra of Patwari and Lisy [*J. Chem. Phys. A* **2007**, *111*, 7585]. The experimental spectra feature a substantial spread in CH stretch vibration frequencies due to the alkali metal cation binding to select hydrogens of cyclohexane. This spread was observed to increase with decreasing metal ion size. Exploring the potential energy landscape revealed the presence of three conformers whose energy minima lie within ~ 1 kcal of each other. It was determined that in all conformers the metal ion interacts with three hydrogen atoms; these hydrogen atoms can be either equatorial or axial. The corresponding spectra for these conformers were obtained with a theoretical model Hamiltonian [*J. Chem. Phys.* **2013**, *138*, 064308] that consists of local mode CH stretches bilinearly coupled to each other and Fermi coupled to lower frequency modes. Frequencies and coupling parameters were obtained from electronic structure calculations that were subsequently scaled on the basis of previous studies. Theoretical spectra of a single low energy conformer were found to match well with the experimental spectra. The relative frequency shifts with changing metal ion size were accurately modeled with parameters generated by using $\omega\text{B97X-D/6-311++(2d,p)}$ calculations.



INTRODUCTION

The influence of intermolecular interactions on the CH stretch in alkanes and substituted alkanes can lead to a wide range of frequency shifts to both lower and higher frequencies. Of particular interest is the interaction that involves closed shell monovalent ions. Even for the simplest single-carbon species, the differences can be striking. For halide ions interacting with methane, the binary complexes take on an η_1 configuration with a single CH directed toward the halide. In the case of F^- , this leads to a shift in the vibrational frequency of -380 cm^{-1} from the ν_1 band of free CH_4 , while the nonbonded CH groups are slightly shifted by -60 cm^{-1} from the ν_3 band of free CH_4 .^{1,2} The magnitudes of the shift decrease with increasing halide radii (or alternatively, decreasing halide charge density), reflecting a weakening of the intermolecular interaction.^{1,3,4} Replacing the halide ion with an alkali metal cation results in a different binding pattern, an η_3 configuration, with the ion approaching along the C_{3v} face interacting directly with three CH groups simultaneously. For $\text{Li}^+(\text{CH}_3)_3\text{Ar}$, the two infrared active stretching modes associated with these groups are found at a ν_1 band at 2859 cm^{-1} and a $\nu_3(\text{e})$ band at 2965 cm^{-1} . The remaining CH group, which is on the opposite side and points away from the ion, has a stretching band, $\nu_3(\text{a}_1)$, near 3025 cm^{-1} .⁵ For the interacting CH groups, the vibrational bands are

shifted, -58 and -54 cm^{-1} , from the ν_1 and ν_3 bands of free CH_4 , respectively, while the noninteracting CH group has a band shifted $+6 \text{ cm}^{-1}$ from the ν_3 band of free CH_4 . Making a change from methane to methyl bromide leads to a very different result. The reaction of $\text{Cl}^- + \text{CH}_3\text{Br}$ is the well-known $\text{S}_\text{N}2$ reaction, where the chloride approaches methyl bromide along the C_{3v} face, opposite to the bromine, interacting with the three CH groups. An experimental study of the gas-phase $\text{Cl}^-(\text{CH}_3\text{Br})\text{Ar}_3$ cluster ion observed two infrared (IR) bands in the CH stretching region at 3063 and 3175 cm^{-1} .⁶ These correspond to the ν_1 and ν_4 bands of CH_3Br but are shifted by $+91$ and $+119 \text{ cm}^{-1}$ from the bands of free CH_3Br at 2972 and 3056 cm^{-1} , respectively. This is directly opposite to the influence that halides have on CH stretches in methane.

There has also been substantial theoretical interest in understanding the origin of the frequency shifts involving CH groups, in the context of hydrogen bonding. Of particular interest has been the investigation of what is often called improper, blue-shifting intermolecular hydrogen bonds.⁷ In contrast to conventional hydrogen-bonding, where the red shift

Received: August 1, 2015

Revised: September 15, 2015

Published: September 16, 2015



is due to the weakening of the C–H bond by electron density transfer, the improper blue-shifting hydrogen bond is a result of a structural reorganization induced by electron density transfer from the donor to a remote part of the acceptor.⁷ Efforts to provide a unified picture of hydrogen bond interactions have focused on the electron density distribution and the electron affinity of the atoms involved in the donor. The nature of this distribution determines when the donor hydrogen bond is proper or improper.⁸

In an earlier experimental study of $M^+[\text{cyclohexane}]\text{Ar}$, $M = \text{Li, Na and K}$, gas-phase infrared predissociation (IRPD) spectra displayed a wide spread in the C–H stretch vibrational frequencies, due to the binding of the alkali metal cation. The frequency shifts were to both higher and lower frequencies when compared to the free C–H bands in cyclohexane (cyH).⁹ The magnitudes of the shift decrease with increasing alkali metal cation radii (or alternatively, decreasing cation charge density), reflecting a weakening of the intermolecular interaction, and were analyzed assuming an η_3 configuration, along the S_6 symmetry axis of cyclohexane. Previous theoretical studies suggested two stable structures, the η_3 configuration and a somewhat in-plane configuration where the Li^+ is perpendicular to a C–C bond, that were of comparable energy, 70 kJ/mol.¹⁰ An experimental measurement of the binding energy was somewhat greater, 100 kJ/mol,¹¹ placing it within the range of the cation– π interaction between Li^+ and benzene (134 kJ/mol).¹² Analysis of electrostatic and induction contributions to the binding energy indicated that the contribution from the electrostatic interaction in the η_3 configuration was negligible, with the induction energy being the dominant contributor for Li^+ complexed to cyclohexane.¹³ A recent and extensive study of a number of closed-shell cations with alkanes and alkenes confirmed the importance of the induction component.¹⁴

The IRPD spectra of the $M^+[\text{cyH}]\text{Ar}$, $M = \text{Li, Na, and K}$, systems⁹ offer an opportunity to analyze the spread and distribution of C–H bands, by using a model Hamiltonian that has proven useful in the interpretation of alkyl CH stretches.^{15–18} In this paper we apply this Hamiltonian to these systems. We find excellent agreement with experimental spectra. Our investigation has led to a reassessment of the binding configurations of the alkali metal cations to cyclohexane where three unique η_3 configurations were identified. Of these three, only one appears to be consistent with the experimental spectra and serves as the basis for analysis with the model Hamiltonian.

CALCULATIONS

To model the spectra of the $M^+[\text{cyH}]\text{Ar}$ species, we investigated the potential energy landscape and found three low energy conformers. These conformers, shown in Figure 1, are η_3 conformers in which the ion is approximately equidistant from three hydrogens. The distinguishing feature of these conformers is whether the hydrogens are equatorial or axial. In the two equivalent *aaa* structures the metal ion is equidistant from three axial hydrogens and the conformer has C_{3v} symmetry. There are 6 equivalent *aea* conformers. Here the two axial hydrogens have identical environments because the structure has C_s symmetry. There are also six minima corresponding to the *eae* conformer. This conformer has C_1 symmetry due to the inequivalent environments of the two equatorial hydrogens.

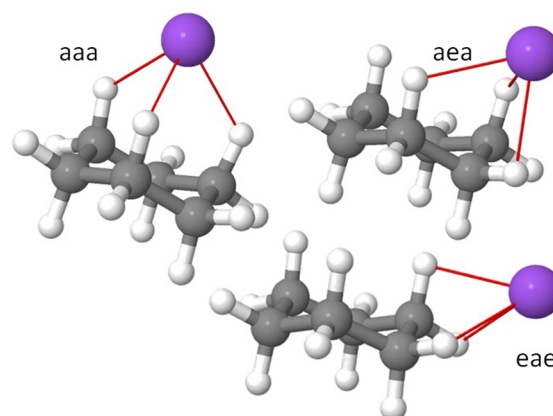


Figure 1. Local minima calculated for the three conformers of the $M^+[\text{cyH}]\text{Ar}$ species. All conformers have three hydrogens approximately equidistant from the metal ion. These hydrogens are labeled as *e* for equatorial and *a* for axial.

The relative stabilities of the conformers are shown in Figure 2. The energies have been calculated by using Gaussian09¹⁹

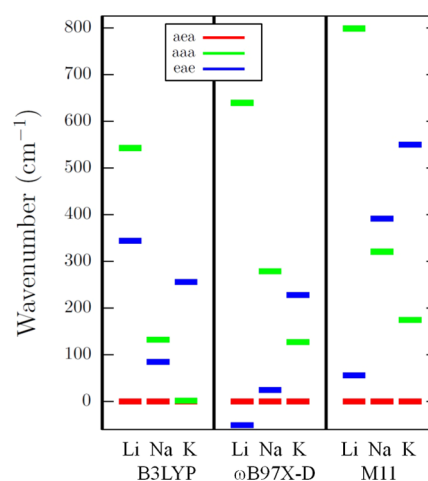


Figure 2. Local minima calculated for the three conformers of the $M^+[\text{cyH}]\text{Ar}$ species of Figure 1. The three panels correspond to (left) B3LYP/6-311+(d,p), (center) $\omega\text{B97X-D}/6-311++(2d,p)$, and (right) M11/6-311++(2df,2p).

with density functional theory with the three functionals^{19–21} indicated in the figure caption. We chose to use the B3LYP functional because our previous studies on CH stretches had used this functional. However, as the systems studied here contain noncovalent interactions, we also used the M11 and $\omega\text{B97X-D}$ functionals, the latter of which includes empirical dispersion corrections. Both of these latter functionals have been previously shown to perform well in terms of binding energetics when compared to CCSD(T)/CBS results on noncovalent systems.²⁰ All minima are measured with respect to the *aea* minima for a given metal, this being the lowest in all cases but one. The barriers between the minima are relatively high, the lowest being the one between two equivalent *eae* minima. Here the transition state, which has C_s symmetry, is calculated to be 260 and 348 cm^{-1} above the *eae* minima as calculated at the B3LYP/6-311+(d,p) and $\omega\text{B97X-D}/6-311++(2d,p)$ levels, respectively. The *aea* minima are also found to be the most stable at the MP2 level of theory with the 6-311+(d,p) basis for all the metals. The relative energies of the *eae*

conformer, $E_{eae} - E_{aea}$ are 480, 54, and 71 cm^{-1} for Li, Na, and K, respectively. The corresponding relative energies of the *aaa* conformer are 584, 348, and 348 cm^{-1} , respectively

The infrared spectra, calculated in the normal mode-linear dipole limit, for the three conformers are quite different in the CH stretch alkyl stretch region. These spectra, along with the experimental IRPD spectrum for $\text{Na}^+[\text{cyH}]\text{Ar}$ are shown in Figure 3. The most dramatic observed effect due to the ion is

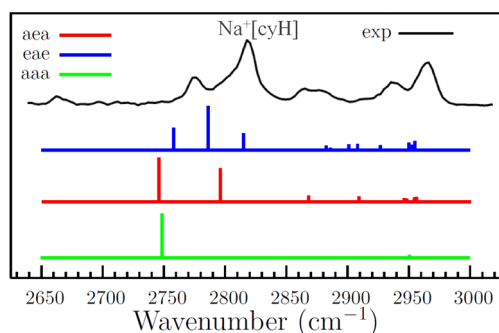


Figure 3. Comparison of IRPD spectra of $\text{Na}^+[\text{cyH}]\text{Ar}$ and scaled normal mode spectra of the three conformers of Figure 1. Calculations carried out at the B3LYP/6-311+(d,p) level and frequencies are scaled by 0.9595.

the presence of the intense transitions below 2850 cm^{-1} . The normal mode calculations also predict such transitions, but the number of these transitions is different for each conformer. The intensities as well as frequencies of these transitions are reported in Table 1. Also shown is the result of a calculation

Table 1. Select CH Stretch Vibrational Frequencies (cm^{-1}) and Intensities (km/mol)^a for the $\text{Na}^+[\text{cyH}]$ Conformers of Figure 1

<i>aaa</i>		<i>eae</i>		<i>aea</i>		<i>aea-Ar</i>	
freq	int	freq	int	freq	int	freq	int
2723	8	2757	94	2736	5	2741	4
2723	8	2786	184	2746	223	2751	218
2748	536	2815	70	2796	169	2799	175

^aB3LYP/6-311+G(d,p) frequencies scaled by 0.9595.

that includes the Ar atom that is used in the IRPD tagging. For the *eae* geometry the largest effect on the vibrational frequencies is a 5 cm^{-1} red shift of the lowest frequency mode. On the basis of this result, the presence of the Ar is henceforth ignored.

The normal mode spectra can be readily understood in terms of reduced dimensional CH stretch local mode Hamiltonians. The red shifts of the three CH stretches that are proximal to the metal ion are sufficiently large that they decouple from the remaining CH stretches. The associated 3×3 CH stretching Hamiltonians of the three conformers are shown below.

$$\mathbf{H}_{\text{CH}}^{\text{aaa}} = \begin{pmatrix} 2733 & & \\ 9 & 2733 & \\ & 9 & 2733 \end{pmatrix} \quad (1)$$

$$\mathbf{H}_{\text{CH}}^{\text{eae}} = \begin{pmatrix} 2791 & & \\ -15 & 2806 & \\ 9 & 8 & 2764 \end{pmatrix} \quad (2)$$

$$\mathbf{H}_{\text{CH}}^{\text{aea}} = \begin{pmatrix} 2744 & & \\ 9 & 2793 & \\ 7 & 9 & 2744 \end{pmatrix} \quad (3)$$

Focusing on the *aea* conformer, we expect to see three low energy CH stretch states whose energies can be described by diagonalizing the Hamiltonian of eq 3. The lowest energy fundamental can be described as the antisymmetric linear combination of the two *a* CH local basis states with transition energies of 2744 cm^{-1} . It has an energy of 2737 cm^{-1} . The symmetric linear combination has an energy of 2747 cm^{-1} . The *e* state is slightly shifted from its zero-order position; its energy is 2796 cm^{-1} . This simple picture agrees well with the full normal mode scaled (0.9595) results of Table 1.

We now turn to a consideration of the intensities of the transitions reported in Table 1. The dipole derivative vectors for the CH stretch coordinates approximately point along the CH bonds. Because the *a* bonds of the chair are nearly parallel, this leads to the oscillator strength of symmetric stretch state at 2746 cm^{-1} being 40 times greater than that of the oscillator strength of antisymmetric stretch state at 2736 cm^{-1} as shown in Table 1. For this reason the *aea* conformer appears to have two rather than three red-shifted bright states.

Similar reasoning can be used to understand the spectra of the other conformers. The *eae* conformer has three bright states in the harmonic limit, because the two *e* CH stretch vibrations coupled to the metal ion are not parallel to one another, and because these two local stretches are no longer in equivalent environments. Their site energies (see eq 2) are 2791 and 2806 cm^{-1} , respectively. Finally, for the same reasons, only the symmetric stretch fundamental of the *aaa* conformer carries appreciable oscillator strength.

Comparing the normal mode results to the experimental spectrum, we see that only the *aea* spectrum has the two main peaks that are red-shifted. Apparently, the high symmetry *aaa* conformer's spectrum contains many fewer lines than the experimental spectrum. We also know, however, that Fermi coupling to low frequency modes can dramatically affect spectral features of the CH alkyl stretches. For this reason we have carried out a calculation that includes these terms.

MODEL HAMILTONIAN RESULTS

The model Hamiltonian being considered has been described in several previous publications,^{15–18} so our description here is brief. The starting point is a normal mode calculation at the B3LYP/6-311+(d,p) level. We transform the Hessian, expressed in Cartesian coordinates, via a series of perturbative transformations²² for the stretches and an orthogonal transformation¹⁸ for the case of the scissors to obtain localized vibrations. These transformations lead to a Hamiltonian that consists of the local CH stretches, scissors, and if appropriate, other low frequency vibration modes. In the present study the other modes of relevance are the CH_2 wagging modes.

Diagonalization of either the scissor or CH stretch local mode Hamiltonians lead to results that, to within 1.0 cm^{-1} , are the same as the full normal mode results. The local CH stretches are scaled by 0.9595 and the scissors and other low frequency modes by 0.975. An anharmonicity for the scissor vibrations is included so that the overtones of the scissor modes are red-shifted by 9 cm^{-1} from the combination bands, a value that comes from perturbative calculations carried out on deuterated ethane.¹⁷ The scissor scaling came from a fit of

methyl stretches.¹⁷ The scaling of the stretching vibration was obtained from fitting a $-\text{CH}_2-\text{CH}_2-$ spectrum and is a value that has been used in all our previous studies. The Fermi couplings are calculated by using finite differences. There are both potential and kinetic contributions in our curvilinear coordinate calculations. We used a scaling of 0.72, this leading to a 22 cm^{-1} Fermi coupling matrix element for the chair form of cyclohexane, which is consistent with values found in previous studies. Dipole derivatives are unscaled.

The results of these calculations are reported in Figure 4. The intense CH stretches of the *aaa* conformer are so red-

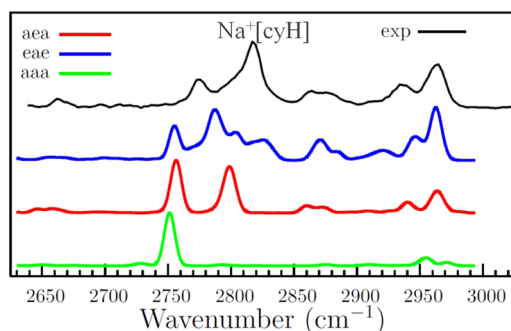


Figure 4. Comparison of IRPD spectra of $\text{Na}^+[\text{cyH}][\text{Ar}]$ to results of model Hamiltonian spectra of the three conformers of Figure 1. Calculations carried out at the B3LYP/6-311+(d,p) level. All spectra are normalized so that the largest peak has the same height. Transitions are broadened with a Gaussian line shape $N \exp[-\alpha^2(\omega - \omega_i)^2]$, where $\alpha = 9.0\text{ cm}^{-1}$.

shifted that the normally important scissor overtones do not noticeably affect the spectrum. The local scissor frequencies for the *aaa* conformer are either 1455 or 1467 cm^{-1} , where the higher frequency corresponds to the three local scissors whose hydrogens are close to the cation. Whereas the *aaa* conformer has too few lines, the *eae* conformer appears to have too many. Of the three spectra, the spectrum of the *aea* conformer is most similar to the experimental spectrum. In all cases, however, the low energy peaks appear to be too red-shifted compared to the experiment.

Before proceeding, it is important to note that there are alternative mechanisms that can lead to additional lines. If the low frequency modes of the metal ion are sufficiently coupled to the CH stretches, one can observe excitation to combination bands consisting of one quantum of CH stretch excitation plus one quantum of excitation of the low frequency cation mode. For the *aaa* conformer there is a degenerate bending mode with a frequency of 94 cm^{-1} and a metal stretch mode at 102 cm^{-1} . To test whether such combination bands would be observed here, we studied select low dimensional Hamiltonians for all the conformers. The Hamiltonians included the three red-shifted CH stretches plus the three low frequency metal ion modes. Potential energy force fields including up to sixth-order terms and dipole moment expansions including up to second-order terms were developed. The corresponding kinetic energy operators were obtained so that the vibrational eigenstates and their transition intensities could be calculated. The results of these calculations clearly showed that the combination modes involving the low frequency modes do not play a role.

As is evident from the results of Figure 4, the B3LYP calculations appear to overly red shift the lines. Having examined a wide range of possible vibration interactions that

could be the cause of this, it appears that the shortcoming in the comparison between theory and experiment is due to the electronic structure results. For this reason we investigated whether other functionals would better predict the extent of the red shift due to interactions with metal ion. We considered both the $\omega\text{B97X-D}^{21}$ and M11²⁰ functionals. Normal mode results for these calculations are shown for the *aea* isomer in Figure 5.

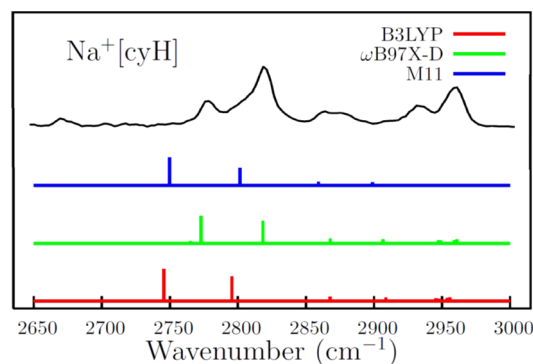


Figure 5. Comparison of IRPD spectra of $\text{Na}^+[\text{cyH}][\text{Ar}]$ to results of model Hamiltonian spectra of the *aea* conformers of Figure 1. Calculations carried out at B3LYP/6-311+(d,p), $\omega\text{B97X-D}/6-311++(2\text{d,p})$, and M11/6-311++(2df,2p) levels.

The $\omega\text{B97X-D}$ functional CH stretch frequencies are scaled by 0.9505. This value was chosen so that the scaled B3LYP and $\omega\text{B97X-D}$ functionals, for the basis sets reported in the figure caption, both yield the same frequencies of the axial CH stretches of the chair conformer of cyclohexane. The lower frequency modes are scaled by 0.9716, this value being chosen so that the scaled B3LYP and $\omega\text{B97X-D}$ functionals yield the same scissor frequency for the chair conformer. One can clearly see that the dispersion-corrected $\omega\text{B97X-D}$ functional appears to provide better agreement for the red-shifted lines.

The two theoretical calculations are compared in more detail in Figure 6, showing frequency results for all three cations as

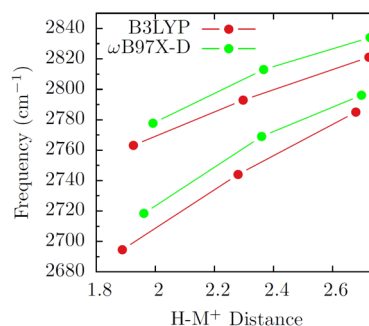


Figure 6. Scaled local CH stretch frequencies for the *aea* conformer of $\text{M}^+[\text{cyH}][\text{Ar}]$ species for $\text{M} = \text{Li, Na, K}$. Four leftmost (rightmost) points correspond to Li (K). Top (bottom) two lines correspond to equatorial (axial) stretches.

functions of distance between the ion and the hydrogen. One sees that the CH stretch frequencies roughly scale linearly with the metal–hydrogen bond distance, with the equatorial CH stretching being higher in frequency. The differences between the two functionals increase as the metal–hydrogen interaction increases.

The scaling behavior shown in Figure 6 highlights the primary effect needed for understanding the full spectral range for this series of metal cations, a strong red shift in CH frequency as a result of the H–M⁺ interactions. Before proceeding, however, a secondary effect of the metal should also be noted. In Figure 7, we compare CH stretch frequencies

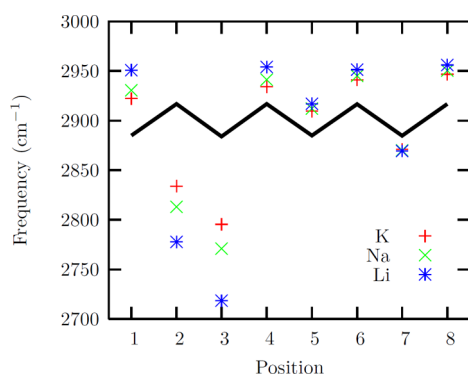


Figure 7. Eight unique CH stretch site frequencies of the local mode Hamiltonian for the *aea* conformer for M = Li, Na, and K as a function of position on the ring. Frequencies were calculated at the ω B97X-D/6-311++(2d,p) level and scaled by 0.9505. Position numbers are odd for axial and even for equatorial CH groups and increase going around the ring. Sites 1 and 2 correspond to the H's on the CH₂ group whose equatorial H interacts with the metal ion. Sites 3 and 4 correspond to the H's on the CH₂ group whose axial H interacts with the metal ion. The black line corresponds to cyclohexane results. The strong red shifts are observed at positions 2 and 3, these corresponding to the equatorial and axial stretches vicinal to the metal. Almost all other sites are blue-shifted. The magnitude of the shift increases as the M⁺–H distances decrease.

for the various positions on the cyclohexane ring. The red shifts observed for positions 2 and 3 have been considered. Note, the second of the two red-shifted axial sites is not included, as the figure includes only the symmetry unique results. The additional feature observed here is a blue shift in the remaining site frequencies. These shifts, which are as large as +40 cm^{−1}, can be compared to the +6 cm^{−1} shift for the noninteracting CH in the Li⁺(CH₄)Ar complex in which the three interacting CH groups are red-shifted.⁵ It can be seen in the figure that this shift increases as the H–M⁺ distance decreases. With these two effects in mind, we now turn to the spectral results.

Theoretical spectra based on the model Hamiltonian are compared to IPRD spectra in Figure 8. In contrast to the above results, these results include the Fermi coupling between stretches, scissors, and wagging modes. Given the excellent agreement, we can now confidently interpret the major spectral features that are observed for this series. One notes an increasing red shift as one moves up the figure. The model Hamiltonian ingredient that accounts for this shift is the CH stretch frequency shift displayed in Figure 6. Also observed is a blue shift at the higher end of the spectrum. This too is well produced by the model.

The majority of the shifts in the broad features in the spectra can be explained in the normal mode limit. In the context of our model, this limit is obtained when the Fermi couplings are set to zero. In this limit we find that all the main peaks remain except for the lowest energy peak observed for the lithium ion. This peak is due to the coupling to the overtone to the out-of-plane wag whose fundamental frequencies are centered about 1340 cm^{−1}.

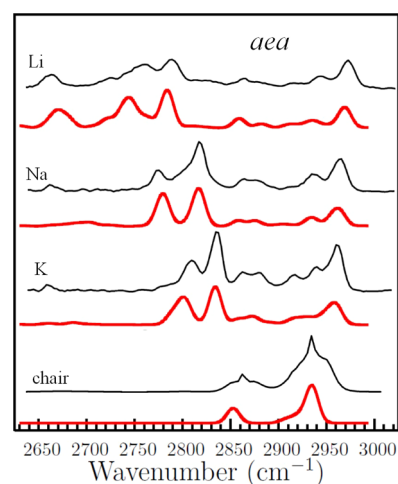


Figure 8. Comparison of IRPD spectra of M⁺[cyH][Ar] (black) to results of model Hamiltonian spectra (red) of the *aea* conformers of Figure 1. Bottom panel compares spectra of the chair conformer of cyclohexane. Calculations carried out at ω B97X-D/6-311++(2d,p). Transitions are given a Gaussian line shape $N \exp[-(\omega - \omega_i)^2/\alpha^2]$, where $\alpha = 9.0$ cm^{−1}.

Although the role of Fermi couplings is not pronounced in Figure 8, it is clearly apparent if one makes the comparison at higher resolution. This comparison is made in Figure 9. Two

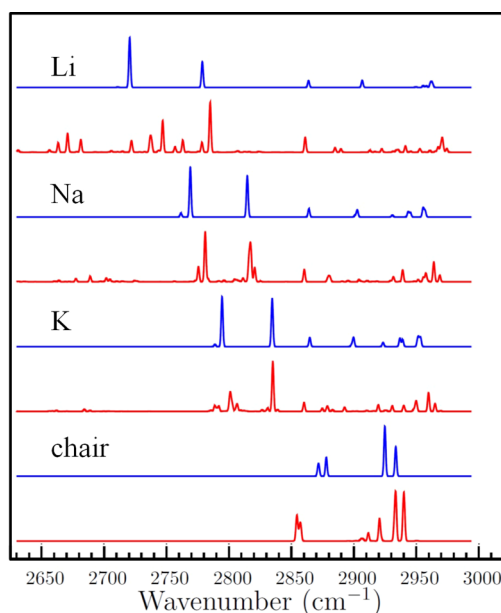


Figure 9. Comparison of normal mode spectra (upper, blue) to the model Hamiltonian spectra (lower, red) of the *aea* conformer of M⁺[cyH] for M = Li, Na, K, plus the chair conformer without the cation. Calculations were carried out at the ω B97X-D/6-311++(2d,p) level. CH stretch frequencies are scaled by 0.9505 and lower frequencies scaled by 0.9716. Transitions are broadened with a Gaussian line shape $N \exp[-(\omega - \omega_i)^2/\alpha^2]$, where $\alpha = 1.0$ cm^{−1}.

spectra are shown for each of the *aea* conformers. They correspond to the scaled normal mode result (upper) and the model Hamiltonian result (lower) of Figure 8 but at higher resolution. Many of the additional lines are due to vibrations involving out-of-plane wags. There are many combination states consisting of one quantum excitation of the out-of-plane

CH₂ wags and one quantum of scissor vibration, whose zero-order energies lie near 2800 cm⁻¹, and many wag overtones at lower frequencies. The combination states are more weakly coupled to the CH stretch fundamentals than are the overtone states. For the localized vibrations involving the axial CH stretch coupling to the contiguous bending vibrations we find 28, 11, and 34 cm⁻¹ wavenumber couplings to the overtone of the scissor, combination of the scissor and wag, and the overtone of the wag, respectively. Interestingly, not only does the cation red shift the stretch frequency but it also increases the coupling to the scissor modes. The 28 cm⁻¹ value for the scissor coupling is greater than the 21–22 cm⁻¹ found in the absence of the metal ion.

CONCLUSIONS

We have described and reported the theoretical results for alkyl CH stretch spectra of various conformers of M⁺[cyH] species for M = Li, Na, K. The model includes Fermi coupling to nearly degenerate scissor modes. The experimental IRPD spectra⁹ are assigned to the *aea* conformer on the basis of agreement with the computed number and distribution of the spectral features. This result is consistent with the results of electronic structure calculations based on density functional and MP2 levels of theory. The excellent agreement between theory and experiment enables us to analyze confidently the spread and distribution of the local C–H stretch frequencies that arise as a result of interactions with the metal ion.

This study is part of an ongoing research effort to improve our ability to extract information from the alkyl CH stretch region of IR spectra. This work has shown that the model has sufficient predictive power to distinguish between different low energy conformers. By considering metal interactions, this work has extended our previous studies^{15–18} to include interactions that significantly shift (~150 cm⁻¹) the CH stretch fundamental transitions. We find that the ω B97X-D functional provided a more accurate description of these shifts than does the B3LYP functional.

The surprisingly strong interaction between the metal cations and the CH groups indicates that the hydrogen bond interaction in the η_3 configuration for the *aea* conformer is much stronger than the η_3 configuration between the same ions and methane. The larger separation between the individual CH groups in cyclohexane versus methane appears to facilitate the weakening of the C–H bond by Li⁺, as manifested by frequency shifts on the order of –100 cm⁻¹ for cyclohexane as compared to the –50 to –60 cm⁻¹ for methane. Some evidence for structural reorganization induced by electron density transfer is also present, with blue shifts of up to 40 cm⁻¹ for some CH groups in the Li⁺–cyH system without the presence of either delocalized electrons (as is the case in alkenes) or heavy atoms (as in the case of the alkyl halides). Though not as large as the +90 and +120 cm⁻¹ shifts in the Cl–(CH₃Br)Ar₃ system, it is ~10 times larger than that observed for Li⁺(CH₄)Ar. The identification of the *aea* conformer as the experimentally observed species has also encouraged us to consider larger cluster sizes with up to four cyclohexanes to test the potential of this molecule to serve as a selective solvent for Li⁺, taking our earlier investigation (ref 9) in a new direction.

AUTHOR INFORMATION

Corresponding Author

*E. L. Sibert. E-mail: elsibert@wisc.edu.

Notes

The authors declare no competing financial interest.

ACKNOWLEDGMENTS

E.L.S. and D.P.T. gratefully acknowledge support from NSF under grant number [CHE-1213449]. J.M.L. acknowledges that this material is based on work partially supported by the National Science Foundation under grant number [CHE-1124821], and while serving at the National Science Foundation.

REFERENCES

- (1) Wild, D.; Loh, Z.; Bieske, E. Infrared Spectra of the F⁻-CH₄ and Br⁻-CH₄ Anion Complexes. *Int. J. Mass Spectrom.* **2002**, *220*, 273–280.
- (2) Loh, Z. M.; Wilson, R. L.; Wild, D. A.; Bieske, E. J.; Lisy, J. M.; Njegic, B.; Gordon, M. S. Infrared spectra and ab initio calculations for the F-(CH₄)_n (n = 1–8) anion clusters. *J. Phys. Chem. A* **2006**, *110*, 13736–13743.
- (3) Wild, D.; Loh, Z.; Wolynec, P.; Weiser, P.; Bieske, E. The Cl-CH₄ Anion Dimer: Mid Infrared Spectrum and Ab Initio Calculations. *Chem. Phys. Lett.* **2000**, *332*, 531–537.
- (4) Loh, Z.; Wilson, R.; Wild, D.; Bieske, E.; Gordon, M. Infrared Spectra and Ab Initio Calculations for the Cl⁻-CH_{4n} (n = 1–10) Anion Clusters. *J. Phys. Chem. A* **2005**, *109*, 8481–8486.
- (5) Rodriguez, O., Jr.; Lisy, J. M. Infrared Spectroscopy of Li⁺(CH₄)_nAr_m, n = 1–6, Clusters. *J. Phys. Chem. A* **2011**, *115*, 1228–1233.
- (6) Ayotte, P.; Kim, J.; Kelley, J.; Nielsen, S.; Johnson, M. Photoactivation of the Cl⁻+CH₃Br S_N2 Reaction via Rotationally Resolved C-H Stretch Excitation of the Cl⁻-CH₃Br Entrance Channel Complex. *J. Am. Chem. Soc.* **1999**, *121*, 6950–6951.
- (7) Hobza, P.; Havlas, Z. Blue-shifting Hydrogen Bonds. *Chem. Rev.* **2000**, *100*, 4253–4264.
- (8) Joseph, J.; Jemmis, E. D. Red-, blue-, or no-shift in hydrogen bonds: A unified explanation. *J. Am. Chem. Soc.* **2007**, *129*, 4620–4632.
- (9) Patwari, G. N.; Lisy, J. M. Cyclohexane as a Li⁺ Selective Ionophore. *J. Phys. Chem. A* **2007**, *111*, 7585–7588.
- (10) Gadre, S.; Pingale, S. Polarization-corrected Electrostatic Potential for Probing Cation Binding Patterns of Molecules. 1. Saturated Hydrocarbons. *J. Am. Chem. Soc.* **1998**, *120*, 7056–7062.
- (11) Staley, R.; Beauchamp, J. Intrinsic Acid-Base Properties of Molecules - Binding-Energies of Li⁺ to π -donor and *n*-Donor Bases. *J. Am. Chem. Soc.* **1975**, *97*, 5920–5921.
- (12) Kim, D.; Hu, S.; Tarakeshwar, P.; Kim, K.; Lisy, J. Cation- π Interactions: A Theoretical Investigation of the Interaction of Metallic and Organic Cations with Alkenes, Arenes, and Heteroarenes. *J. Phys. Chem. A* **2003**, *107*, 1228–1238.
- (13) Tsuzuki, S.; Yoshida, M.; Uchimaru, T.; Mikami, M. The Origin of the Cation/ π Interaction: The Significant Importance of the Induction in Li⁺ and Na⁺ Complexes. *J. Phys. Chem. A* **2001**, *105*, 769–773.
- (14) Premkumar, J. R.; Sastry, G. N. Cation Alkane Interaction. *J. Phys. Chem. A* **2014**, *118*, 11388–11398.
- (15) Buchanan, E. G.; Dean, J. C.; Zwier, T. S.; Sibert, E. L. Towards a First-Principles Model of Fermi Resonance in the Alkyl CH Stretch Region: Application to 1,2-Diphenylethane and 2,2,2-Paracyclophane. *J. Chem. Phys.* **2013**, *138*, 064308.
- (16) Buchanan, E. G.; Sibert, E. L.; Zwier, T. S. Ground State Conformational Preferences and CH Stretch-Bend Coupling in a Model Alkoxy Chain: 1,2-Diphenoxyethane. *J. Phys. Chem. A* **2013**, *117*, 2800–2811.
- (17) Sibert, E. L.; Kidwell, N. M.; Zwier, T. S. A First-Principles Model of Fermi Resonance in the Alkyl CH Stretch Region: Application to Hydronaphthalenes, Indanes, and Cyclohexane. *J. Phys. Chem. B* **2014**, *118*, 8236–8245.

- (18) Sibert, E. L.; Tabor, D. P.; Kidwell, N. M.; Dean, J. C.; Zwier, T. S. Fermi Resonance Effects in the Vibrational Spectroscopy of Methyl and Methoxy Groups. *J. Phys. Chem. A* **2014**, *118*, 11272–11281.
- (19) Frisch, M. J.; et al. *Gaussian 09*, Revision A.1; Gaussian Inc.: Wallingford, CT, 2009.
- (20) Peverati, R.; Truhlar, D. G. Improving the Accuracy of Hybrid Meta-GGA Density Functionals by Range Separation. *J. Phys. Chem. Lett.* **2011**, *2*, 2810–2817.
- (21) Chai, J.-D.; Head-Gordon, M. Long-range Corrected Hybrid Density Functionals with Damped Atom-Atom Dispersion Corrections. *Phys. Chem. Chem. Phys.* **2008**, *10*, 6615–6620.
- (22) Sibert, E. L. Dressed Local Mode Hamiltonians for CH Stretch Vibrations. *Mol. Phys.* **2013**, *111*, 2093–2099.